Electrochimica Acta 55 (2010) 2951–2957

Contents lists available at ScienceDirect

Electrochimica Acta

journal homepage: www.elsevier.com/locate/electacta

Microwave solid-state synthesis and electrochemical properties of carbon-free $Li_3V_2(PO_4)_3$ as cathode materials for lithium batteries

Gang Yang*, Haidong Liu, Hongmei Ji, Zhongzhong Chen, Xuefan Jiang

Jiangsu Laboratory of Advanced Functional Material, Department of Chemistry, Changshu Institute of Technology, Nansanhua Road 99, Changshu, Jiangsu 215500, China

ARTICLE INFO

Article history:
Received 9 October 2009
Received in revised form
27 November 2009
Accepted 29 November 2009
Available online 3 December 2009

Keywords:
Lithium secondary batteries
Cathode material
Microwave solid-state synthesis
Electrochemistry

ABSTRACT

Monoclinic $Li_3V_2(PO_4)_3$ can be rapidly synthesized at 750 °C for 5 min (MW5m) by using microwave solid-state synthesis method. The refined cell parameters and atomic coordination of the sample MW5m show some deviations compared with those of the sample synthesized in conventional solid-state synthesis method, especially the coordinate of Li atoms. Compared with the electrochemical properties of the carbon-coating sample $Li_3V_2(PO_4)_3$, the carbon-free sample MW5m presents well electrochemical properties. In the cut-off voltage of 3.0–4.3 V, MW5m sample presents a specific charge capacity of 132 mAh g^{-1}, almost equivalent to the reversible cycling of two lithium ions per $Li_3V_2(PO_4)_3$ formula unit (133 mAh g^{-1}), and specific discharge capacity of 126.4 mAh g^{-1}. In the cut-off voltage of 3.0–4.8 V, MW5m shows an initial specific discharge capacity of 183.4 mAh g^{-1} at 0.1 C, near the theoretical discharge capacity. In the cycle performance, the capacity fade of $Li_3V_2(PO_4)_3$ is dependent on the cut-off voltage and the preparation method, more capacity lost at relatively higher charge/discharge voltage. The reasons for the excellent electrochemical properties of $Li_3V_2(PO_4)_3$ rapidly synthesized in microwave field are discussed in detail.

1. Introduction

Rechargeable lithium-ion batteries are the most important power sources for the increasing demand from portable electronic products, electrical vehicles (EV) and hybrid electrical vehicles (HEV), etc. Lithium cobalt oxide is the first utilized as positive electrode for commercial lithium secondary batteries, but its high cost and toxicity prohibit the use in large-scale applications, such as EV and HEV. In recent years, several cathode materials have been used for the increasing demand of lithium batteries, such as $LiFePO_4$. Another class of cathode materials, transition-metal phosphates, $LiMPO_4$ (M = Ni, Co, Mn), [1–4] $Li_3V_2(PO_4)_3$, [5–13] and $LiVPO_4F$ [14,15] have been proposed as cathode materials for lithium batteries because of their remarkable electrochemical performance and thermal stability. Among the above mentioned phosphates, monoclinic $Li_3V_2(PO_4)_3$ with both mobile Li^+ cations and redox-active metal sites located within a rigid phosphate framework, has received intensive attention for the stable framework, higher operating voltage, and large theoretical capacity. Monoclinic lithium vanadium phosphate contains three independent lithium sites with a theoretical discharge capacity of 197 mAh g^{-1}, while three Li ions are completely extracted at the voltage of 4.8 V [6,9,16,17].

However, the low conductivity of $Li_3V_2(PO_4)_3$ as $LiFePO_4$ degrades its electrochemical performance. It is an effective method to improve the electrochemical performance by using carbon-coating process or the substitution of transition metal in vanadium site [8,11,18–21]. $Li_3V_2(PO_4)_3$ had already been prepared by using hydrogen or carbon as reduction agents [9,22–25]. These synthesis processes need high calcinations temperature and long reaction time.

There are many synthesis methods applied to cathode materials, including conventional solid-state synthesis, hydrothermal, sol–gel and microwave solid-state synthesis methods, etc. The microstructure and property of the materials prepared by different synthesis methods are quite different. Over the past decade, microwave heating has become an important method in chemical synthesis and materials processing. Since the microwave energy is directly absorbed by the sample, uniform and rapid heating can be achieved within several minutes. Microwave solid-state synthesis method has already been applied to synthesize a number of inorganic materials, such as carbides, nitrides, complex oxides, silicides, zeolites, etc. The beneficial results and application have been found with the materials prepared by microwave irradiation, and many researchers have reported the substitution of conventional solid-state synthesis by microwave method [26–33].

Microwave solid-state synthesis method as a novel method has been developed to prepare cathode materials for lithium batteries [27–33]. For instance, Higuchi et al. and Park et al. [28,29] prepare $LiFePO_4$ by using domestic microwave oven. In our previous

* Corresponding author. Tel.: +86 512 52251898; fax: +86 512 52251842.
E-mail address: gyang@cslg.edu.cn (G. Yang).

0013-4686/$ – see front matter © 2009 Elsevier Ltd. All rights reserved.
doi:10.1016/j.electacta.2009.11.102

paper, the heating behavior and crystal growth mechanism of layered compounds, such as the synthesis of cathode material of LiV_3O_8, have been reported. The structure, morphology and the electrochemical performance of LiV_3O_8 have been found that it is dependent on the microwave irradiation condition [27]. However, the microwave synthesis of solid-state materials in lab is mostly done with domestic microwave oven. The irradiation power and the reaction temperature cannot be detected and controlled, i.e., the synthesis process is fully empirical.

In this paper, the carbon-free $Li_3V_2(PO_4)_3$ samples have been synthesized in 5 min by using microwave solid-state synthesis tube furnace. Because the surface temperature of the sample pellet directly detected by an infrared pyrometer, the microwave irradiation power and the reaction temperature are automatically controlled by a computer. The lattice parameter of the rapidly formed $Li_3V_2(PO_4)_3$ crystal in microwave irradiation field is refined, and the electrochemical properties are discussed in detailed.

2. Experimental

2.1. Description of the microwave solid-state reaction system

Scheme 1 shows the temperature-controlled microwave solid-state synthesis tube furnace (frequency 2.45 GHz, maximum power 2 kW, multimode oven). A water-cooled multimode cavity consists of a quartz tube ensuring a controlled atmosphere. The surface temperature of the sample during irradiation process is directly monitored online by an infrared pyrometer (Raytek, Marathon series) connected with a computer. The heating rate keeps at about 60 °C/min and the reaction temperature is automatically controlled by the input irradiation power. The accuracy of temperature recorded by this system is generally within ±1 °C over the whole range of heating. About 3 g reactants pellet is placed in the center of an alumina tube. The alumina tube is placed inside a well-insulated kaowool cannula to avoid the broken of the quartz tube upon the high-temperature surrounding.

2.2. Preparation of carbon-free $Li_3V_2(PO_4)_3$

Pure $Li_3V_2(PO_4)_3$ is synthesized using V_2O_5, $NH_4H_2PO_4$, Li_2CO_3, and oxalic acid as starting materials. Oxalic acid is used here as a chelating agent and reducing agent. First, oxalic acid and V_2O_5 in a stoichiometric ratio are dissolved in deionized water at 70 °C. After a clear blue solution formed, a mixture of stoichiometric $NH_4H_2PO_4$ and Li_2CO_3 is added to the solution while stirring for 4 h, and then a gel formed at 70 °C. After the gel is dried at 70 °C, pressed into pellets at the pressure of 5 MPa, and then decomposed at 350 °C in an argon atmosphere for 4 h. The obtained precursor is ground and pressed into two pellets under the pressure of 10 MPa. One pellet is heated in a convention furnace at 750 °C for 10 h in flowing argon (the product named as CP10h). The other pellet is reacted at 750 °C for 5 min in flowing argon by using microwave tube furnace (the product named as MW5m). After solid-state synthesis, the as-synthesized samples are cooled to room temperature in the microwave oven.

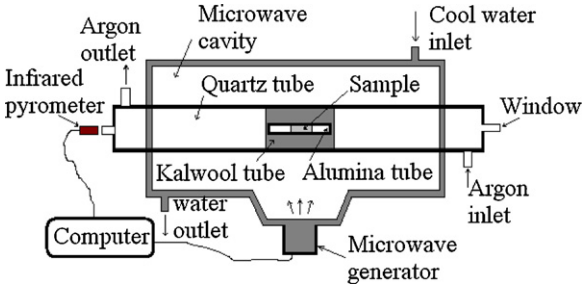

Scheme 1. Diagram of the microwave solid-state synthesis system.

2.3. Sample characterization

All X-ray studies are done on a Rigaku diffractometer with Cu K_α radiation at 40 kV and 30 mA. The diffraction data are collected for 4 s at each 0.02° step width over 2θ ranging from 10° to 80°. The crystal structure parameters of the sample $Li_3V_2(PO_4)_3$ are refined by Rietveld analysis using the General Structure Analysis System (GSAS) [34]. The scanning electron microscope (SEM) is done with Hitachi X650 microscope (20 kV).

2.4. Electrochemical testing

Cyclic voltammetry (CV) is conducted on a PARSTAT 2273 electrochemical workstation. The CV curves for the above test cells are recorded in a potential range of 3.0–4.5 and 3.0–4.8 V (vs Li^+/Li) at a scan rate of 0.2 mV s^{-1} at 25 °C, respectively. A lithium foil acts as both the counter electrode and reference electrode.

Electrochemical charge–discharge performance of the samples is evaluated in model CR2016 coin cells. The as-prepared sample $Li_3V_2(PO_4)_3$ is mixed with acetylene black and Teflon powder in the weight ratio 80:15:5. Lithium foil is used as the anode, and 1 M $LiPF_6$ in EC:DMC = 1:1 is used as the electrolyte. The separator is Celgard 2300 membrane. Cells are assembled in an argon-filled glove box. Cycling and charge–discharge performances of the testing cells are carried out on Land CT2001A at 0.1 C rate, and the cut-off voltage is controlled at the range of 3.0–4.3 and 3.0–4.8 V vs Li/Li^+, respectively.

3. Results and discussion

Chemical synthesis by microwave heating is very efficient, since it offers rapid volumetric heating, high reaction rates and selectivity, and is energy saving. In the temperature-controlled microwave solid-state synthesis process, the homogeneous heating effects induced by microwave irradiation could create many uniform nucleation centers in the whole sample.

In a typical procedure, V_2O_5 is dissolved in the solution of $H_2C_2O_4$. Oxalic acid is used here as a chelating agent and reducing agent. Oxalic acid and V_2O_5 in a stoichiometric ratio are absolutely reacted. Because the precursor does not contain any carbon source and there is no carbon-coating process following the microwave solid-state synthesis, the as-synthesized $Li_3V_2(PO_4)_3$ samples are carbon free.

The XRD patterns of the samples synthesized for 10 h at 750 °C by using conventional solid-state synthesis method (CP10h), and for 5 min at 750 °C in microwave tube furnace (MW5m) are shown in Fig. 1. The XRD patterns show that all peaks are corresponded to the monoclinic structure of $Li_3V_2(PO_4)_3$ and are similar to the previous reports [10–13]. The diffraction peaks of the sample correspond to a single-phase, and can be indexed as monoclinic structure with a space group of $P2_1/n$.

Upon the same reaction temperature 750 °C, the pure phase of MW5m is rapidly formed in 5 min (as shown in Fig. 1b). By comparison with the relatively long reaction time (about several hours) of $Li_3V_2(PO_4)_3$ formed in conventional solid-state synthesis method, these experimental facts confirm that the crystal growth of $Li_3V_2(PO_4)_3$ lattice could be dramatically accelerated under microwave irradiation field. The lattice structure of MW5m will be affected due to the fast crystal formation.

The XRD pattern refinement of the sample MW5m is shown in Fig. 2. The refined lattice parameters and atomic coordination are listed in Table 1. Because the reliability factor of x^2 is less than 3,

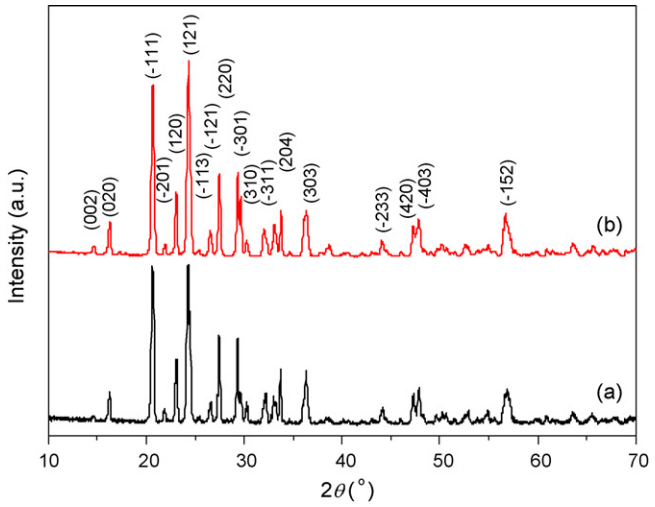

Fig. 1. XRD patterns of $Li_3V_2(PO_4)_3$ synthesized by (a) conventional solid-state synthesis at 750 °C for 10 h and (b) microwave solid-state synthesis at 750 °C for 5 min.

and the weighted factor R_{wp}, R_f and R_p less than 10%, the Rietveld refinement results are reliable. All the Li, V, P, and O atoms occupy Wyckoff position 4e with different coordinates.

The monoclinic unit cell of $Li_3V_2(PO_4)_3$ contains a rigid framework both mobile Li cations and redox-active metal sites located within a phosphate framework sharing oxygen atoms. Each PO_4 tetrahedron is surrounded with four VO_6 tetrahedra, whereas each VO_6 octahedron is surrounded by six PO_4 octahedra. Three lithium ions reside in one tetrahedral site and two pseudotetrahedral sites. The three-dimensional structure allows for reversible extraction/reinsertion of all three lithium ions from the monoclinic structure of vanadium phosphate [9,11,13,21]. Compared with the units of lattice constants of $Li_3V_2(PO_4)_3$ synthesized by conventional solid-state synthesis, MW5m synthesized by microwave rapid synthesis method shows similar results. As shown in Table 1, the fractional coordinates of V and P atoms comprised the rigid framework present small difference between the samples $Li_3V_2(PO_4)_3$ synthesized by conventional and microwave solid-state synthesis, but the three mobile lithium ions show dramatic deviations. For example, the fractional coordinates of Li1(4e) of MW5m are 0.3502(2), 0.3350(1) and 0.2995(2) Å, compared with

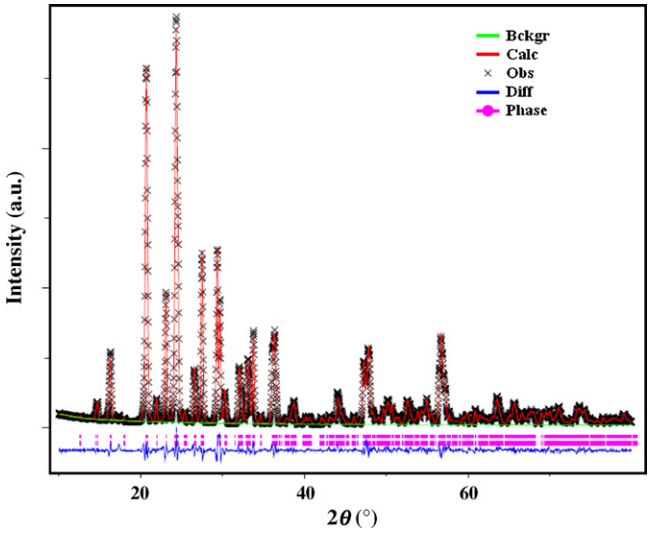

Fig. 2. Rietveld refinement of sample MW5m synthesized at 750 °C for 5 min by using microwave solid-state synthesis method.

Table 1
Atomic sites (number of positions and Wyckoff notation) and fractional coordinates (in units of lattice constants $a = 8.6059(9)$ Å, $b = 12.0359(5)$ Å, $c = 8.5942(2)$ Å and $\beta = 90.5779(2)^\circ$, space group $P2_1/n$) for the sample MW5m. The reliable factors are $R_{wp} = 6.60\%$, $R_p = 4.53\%$, $x^2 = 1.239$, and $R_f = 3.14\%$.

Atom	x	y	z
Li1(4e)	0.3502(2)	0.3350(1)	0.2995(2)
Li2(4e)	0.5638(3)	0.1941(2)	0.4135(3)
Li3(4e)	0.9431(2)	0.2474(2)	0.3300(2)
V1(4e)	0.2479(4)	0.1105(2)	0.4619(6)
V2(4e)	0.7496(4)	0.3900(8)	0.4685(6)
P1(4e)	0.1046(5)	0.1507(7)	0.1040(6)
P2(4e)	0.6094(6)	0.3527(4)	0.1149(6)
P3(4e)	0.0365(5)	0.4932(4)	0.2541(7)
O1(4e)	0.4430(1)	0.3359(6)	0.0792(1)
O2(4e)	0.9287(1)	0.1447(6)	0.1176(9)
O3(4e)	0.3553(1)	0.2667(7)	0.4762(1)
O4(4e)	0.8083(8)	0.2199(6)	0.4922(9)
O5(4e)	0.1741(1)	0.0485(7)	0.0545(1)
O6(4e)	0.6578(1)	0.4721(6)	0.0842(9)
O7(4e)	0.4570(1)	0.0697(7)	0.3713(1)
O8(4e)	0.9257(9)	0.4046(6)	0.3311(8)
O9(4e)	0.1635(1)	0.4318(6)	0.1669(1)
O10(4e)	0.6164(9)	0.0774(5)	0.1278(1)
O11(4e)	0.1642(9)	0.1767(6)	0.2511(1)
O12(4e)	0.6363(9)	0.3232(7)	0.2908(1)

0.292(3), 0.328(2) and 0.298(2) Å of $Li_3V_2(PO_4)_3$ synthesized at high temperature for several hours [9,10]. In these cases, two reasons may be concluded. First, the deviation in the lattice parameters and the atomic coordination is attributed to the strain in the crystal structure as a result of high tension because of the too fast crystal growth process [35]. Second, there is a mismatching of diffusion coefficient of lithium ions and the formation rate of rigid framework by VO_6 octahedra and PO_4 tetrahedra in microwave irradiation field. The VO_6 and PO_4 polyhedra can rapidly form vanadate phosphate frame for several minutes in microwave irradiation field. The detailed crystal growth mechanism of $Li_3V_2(PO_4)_3$ and the relative electrochemical properties of $Li_3V_2(PO_4)_3$ synthesized under different microwave irradiation condition would be discussed in the following paper.

The morphology of $Li_3V_2(PO_4)_3$ particles synthesized at 750 °C for 5 min in microwave irradiation field is confirmed by SEM and TEM examination, and is shown in Fig. 3. In the micrograph, the small particles show good crystallinity and uniformity. The particle size of sample ranged from 1 to 5 μm exhibits a relatively narrow distribution. Due to the homogeneous heating effects and penetrating behavior induced by microwave irradiation, many uniform nucleation centers of the product phase are rapidly created in the whole sample. Many nanoparticles of product are formed in 5 min, and no more time let the particles grow big. As shown in the TEM image, about 100 nm nanoparticles could be seen, but these particles are loose aggregated together.

Several published reports described that $Li_3V_2(PO_4)_3$ samples need carbon coating for good electrochemical performance [8,11,18–21]. In this manuscript, the carbon-free MW5m sample synthesized by microwave solid-state synthesis method presents well electrochemical properties. CV profiles and charge–discharge performances are measured between 3.0 and 4.3, and 3.0 and 4.8 V so as to remove the equivalent of 2 and 3 lithium atoms, respectively.

Cyclic voltammetry is recorded for the sample MW5m using the Li metal as counter and reference electrode in cell configuration, and is shown in Fig. 4. There are three couples of oxidation and reduction peaks between 3.0 and 4.5 V for the sample $Li_3V_2(PO_4)_3$. The three oxidation peaks occurs around 3.67, 3.74 and 4.15 V, and the three reduction peaks are around 3.53, 3.61 and 3.98 V, respectively. The two oxidation peaks around 3.67 and 3.74 V are

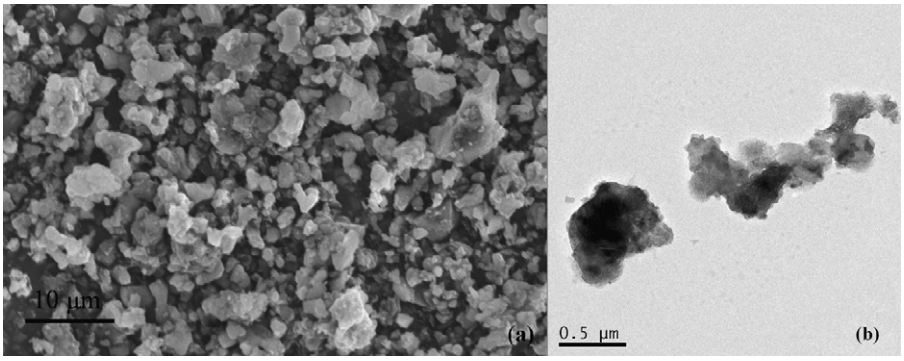

Fig. 3. (a) SEM and (b) TEM images of the sample MW5m synthesized at 750 °C for 5 min by using microwave solid-state synthesis method.

correspond to the removal of the first Li^+ in two steps, because there is an ordered $Li_{2.5}V_2(PO_4)_3$ phase [9,16]. The second Li^+ ion is extracted through one single step around 4.15 V. The two Li^+ ions extraction is also associated with the V^{3+}/V^{4+} redox couple. The above results are in good agreement with those reported by Saidi et al. [16]. During the anodic process, the three peaks located at 3.53, 3.61 and 3.98 V can be attributed to the reinsertion of the two Li^+ ions, associated with the V^{4+}/V^{3+} redox couples. The well-defined peaks and smaller value of potential interval show the good reaction reversibility. The similar redox couples would be concluded in the charge/discharge curves of $Li_3V_2(PO_4)_3$ in the cut-off voltage of 3.0–4.3 V (Fig. 5).

Fig. 5 shows the initial and 30th charge–discharge profiles of the MW5m and CP10h electrode at 0.1 C (13.3 mA/g) at 25 °C in the voltages of 3.0–4.3 V. The carbon-free sample MW5m shows specific charge capacity of 132.0 mAh g^{-1}, almost equivalent to the reversible cycling of two lithium ions per $Li_3V_2(PO_4)_3$ formula unit (133 mAh g^{-1}). The specific discharge capacity of MW5m is 126.4 mAh g^{-1}. The electrode of carbon-free sample CP10h exhibits a reversible specific charge and discharge capacity of 121.1 and 115.5 mAh g^{-1}, respectively.

Three couples of charge/discharge plateaus at 4.09/4.03, 3.70/3.64 and 3.63/3.56 V, are shown in Fig. 5 and corresponded to three compositional regions of $Li_{3-x}V_2(PO_4)_3$ (x = 0–0.5, x = 0.5–1.0 and x = 1.0–2.0), the voltage plateau of each region describes the two-phase transition process in the electrochemical reaction, respectively [5,9]. The three charge–discharge plateaus of the $Li_3V_2(PO_4)_3$ samples of MW5m and CP10h also correspond to the three couples of peaks in the CV profiles, respectively.

$Li_3V_2(PO_4)_3$ contains both mobile Li cations and redox-active metal sites located within a rigid phosphate framework. The thermodynamically stable monoclinic (M) structure, exhibits a complex series of two-phase transitions on Li^+ extraction/reinsertion, followed by a solid solution on lithium reinsertion. For example, the two-phase transition at 3.70/3.64 V belongs to the electrons/Li^+ extracted/reinserted from the V(1) sites [9]. The energies of structures spanning the phase transition are governed by the site potential of the Li^+ ion and their interaction with the V^{n+} ions in the lattice. The capacity at each plateau of the $Li_3V_2(PO_4)_3$ samples is listed in Table 2. There is a significant different plateau capacity of the $Li_3V_2(PO_4)_3$ samples synthesized upon conventional solid-state synthesis and microwave irradiation solid-state synthesis methods, respectively.

The capacity of charge plateaus at 3.62 and 3.70 V is similar in the samples of MW5m and CP10h. However, the specific discharge capacity at plateau 4.03 V of MW5m, the reinsertion process of the phase transition from $LiV_2(PO_4)_3$ to $Li_2V_2(PO_4)_3$, is 61 mAh g^{-1}, but 41 mAh g^{-1} in the sample CP10h. The specific capacity at discharge plateau 3.64 and 3.56 V, the insertion process of the phase transition from $Li_2V_2(PO_4)_3$ to $Li_{2.5}V_2(PO_4)_3$, and $Li_{2.5}V_2(PO_4)_3$ to $Li_3V_2(PO_4)_3$, are almost the same values (as shown in Table 2). As well known, the diffusion constant of Li^+ cation is dependent on the crystal structure of cathode material. For example, the preferential direction of Li^+ cation in olivine crystal structure of $LiFePO_4$ is b axis direction [36,37]. The poor electrochemical properties are mainly caused by the poor ionic/electronic conductivity of $FePO_4$ during the Li^+ insertion/extraction process in the phase transition of $LiFePO_4/FePO_4$. In the charge/discharge process of $Li_3V_2(PO_4)_3$

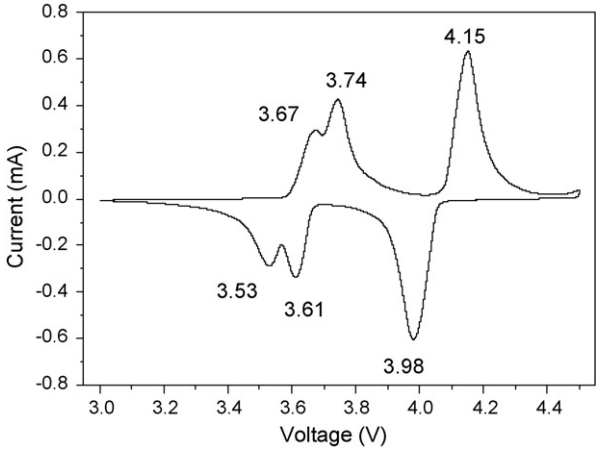

Fig. 4. Cyclic voltammetry of MW5m electrode for the first scanning cycle, in an EC–DEC (1:1) electrolyte cell with Li counter and reference electrodes, and carried out with the scan rate of 0.2 mV s^{-1} between the voltage 3.0 and 4.5 V.

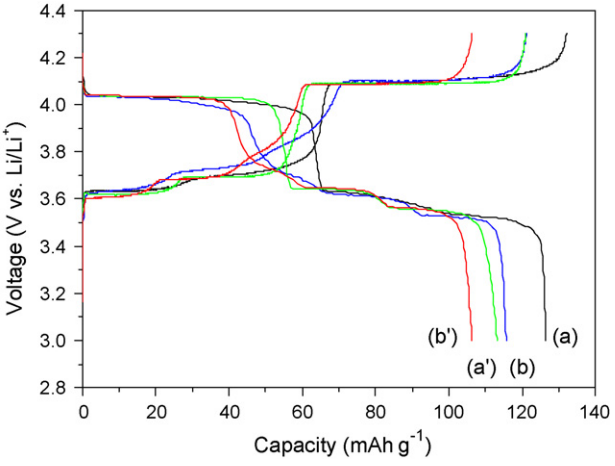

Fig. 5. Charge/discharge profiles of $Li_3V_2(PO_4)_3$ samples in the voltage range of 3.0–4.3 V. (a) The initial and (a′) 30th cycle of MW5m, (b) the initial and (b′) 30th cycle of CP10h.

Table 2
The specific capacity at plateaus for MW5m and CP10h in the first and 30th cycle.

Charge/discharge plateau (V)	MW5m				CP10h			
	Charge (mAh g^{-1})		Discharge (mAh g^{-1})		Charge (mAh g^{-1})		Discharge (mAh g^{-1})	
	1st	30th	1st	30th	1st	30th	1st	30th
4.09/4.03	22	22	61	50	21	16	41	36
3.70/3.64	23	24	22	21	19	17	21	19
3.62/3.56	58	55	23	21	45	40	21	16

in the voltage range of 3.0–4.3 V, three phase transition would be occurred. Based on the specific capacity at the three plateaus, it could be concluded that one key control factor of specific capacity fade would be dependent on the phase transition process between $Li_2V_2(PO_4)_3$ and $LiV_2(PO_4)_3$ during the charge/discharge process of $Li_3V_2(PO_4)_3$ in the voltage range of 3.0–4.3 V. It corresponds with the conclusion published by Nazar's group that the energies of structures spanning the phase transition are governed by the site potential of the Li^+ ion and their interaction with the V^{n+} ions in the lattice [9].

After the 30th charge/discharge cycle, the specific discharge capacity of MW5m decreases about 13 mAh g^{-1}, and the lost discharge capacity is mainly attributed from the irreversible process from $LiV_2(PO_4)_3$ to $Li_2V_2(PO_4)_3$ (as shown in Table 2). The specific discharge capacity of MW5m shows very small degradation after 30 cycles at the plateaus 3.56 and 3.64 V. Similar results appeared in the sample of CP10h. This further confirms the above conclusion that a key control factor of specific capacity fade is dependent on the phase transition process between $LiV_2(PO_4)_3$ and $Li_2V_2(PO_4)_3$ during the charge/discharge process in the voltage range of 3.0–4.3 V.

The cycle performance of the samples MW5m and CP10h in the voltage range of 3.0–4.3 V is shown in Fig. 6. The discharge capacity of MW5m is 126.4 mAh g^{-1} at the first cycle, and decreases to 110.2 mAh g^{-1} (87.2% of initial capacity) after 50 cycles. The sample CP10h presents a low specific discharge capacity than that in the sample MW5m, however relatively better cycle performance is appeared in CP10h. It might be due to the different crystal structure formed under the two synthesized methods. Because MW5m is rapidly synthesized in the microwave irradiation field, the preferential crystal orientation and the tension in the crystal structure would be occurred in the rapid crystal growth process, and might effect the cycleability.

To investigate the extraction/insertion process of the third lithium ion in the sample $Li_3V_2(PO_4)_3$, the CV profile of MW5m in the voltage range of 3.0 and 4.8 V is shown in Fig. 7. Four oxidation and three reduction peaks present in the CV curve. The three oxidation peaks under relatively lower voltages (<4.5 V) and the corresponding three reduction peaks result from the extraction and reinsertion of two lithium ions in $Li_3V_2(PO_4)_3$ as shown in the CV profiles between the voltage ranges 3.0–4.5 V. The oxidation peak at 4.62 V is the extraction of the third Li^+ ion, associated with the phase transition process from $LiV_2(PO_4)_3$ to $V_2(PO_4)_3$. However, there is an absence of the corresponding reduction peak in the CV curves. It is agree with fact that the initial reinsertion of Li^+ cation in $V_2(PO_4)_3$ from a solid solution of two phase [5,9,11]. The relative oxidation/reduction peaks in CVs also appear and correspond to the charge/discharge plateaus of $Li_3V_2(PO_4)_3$ electrode in Fig. 8 at 0.1 C (19.7 mA g^{-1}) and in the cut-off voltage 3.0–4.8 V.

The rapidly synthesized sample MW5m by using microwave solid-state synthesis method presents an initial specific charge capacity of 197 mAh g^{-1}, equivalent to the reversible cycling of three lithium ions per $Li_3V_2(PO_4)_3$ formula unit (197 mAh g^{-1}). The initial specific discharge capacity of MW5m is 183.4 mAh g^{-1} at 0.1 C, higher than the reversible capacity of $Li_3V_2(PO_4)_3$ samples synthesized by means of hydrogen reduction and that of the carbon-coating $Li_3V_2(PO_4)_3$. The $Li_3V_2(PO_4)_3$ sample CP10h synthesized at 750 °C for 10 h, without any carbon-coating process, presents an initial charge and discharge capacity 156.1 and 144.9 mAh g^{-1}, respectively. This indicates that the rapidly formed crystal structure has significant contribution to the improvement on the electrochemical performance of $Li_3V_2(PO_4)_3$.

After dozens of cycles of charge and discharge, the above two samples present a capacity fade shown in Fig. 9. For example, after 50th cycle the discharge specific capacity of MW5m remains 123.7 mAh g^{-1}, and that of CP10h is only 57.3 mAh g^{-1} after 10 cycles. Compared with the good cycleability presented in MW5m and CP10h in the cut-off voltage 3.0–4.3 V (Fig. 6), the significant loss of capacity in the cut-off voltage of 3.0–4.8 V might be due to following reasons. One is the electrolyte oxidation considered

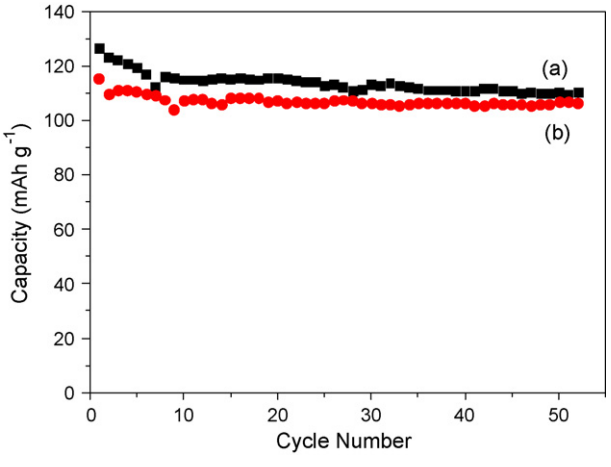

Fig. 6. Cyclic performance of the $Li_3V_2(PO_4)_3$ samples (a) MW5m and (b) CP10h in the voltage range of 3.0–4.3 V.

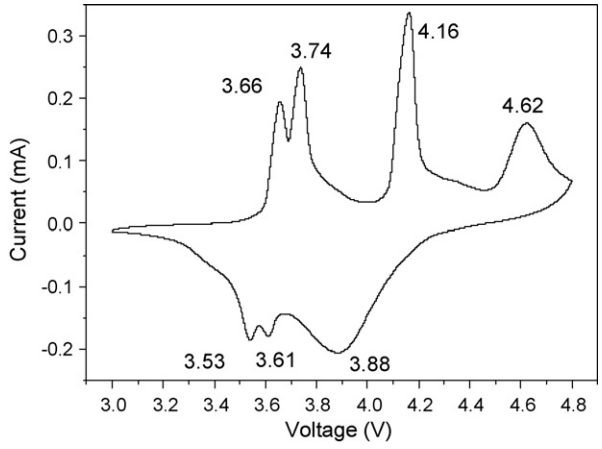

Fig. 7. Cyclic voltammetry of MW5m electrode for the first scanning cycle in an EC–DEC (1:1) electrolyte cell with Li counter and reference electrodes, and carried out at the temperature of 25 °C with the scan rate of 0.2 mV s^{-1} between 3.0 and 4.8 V.

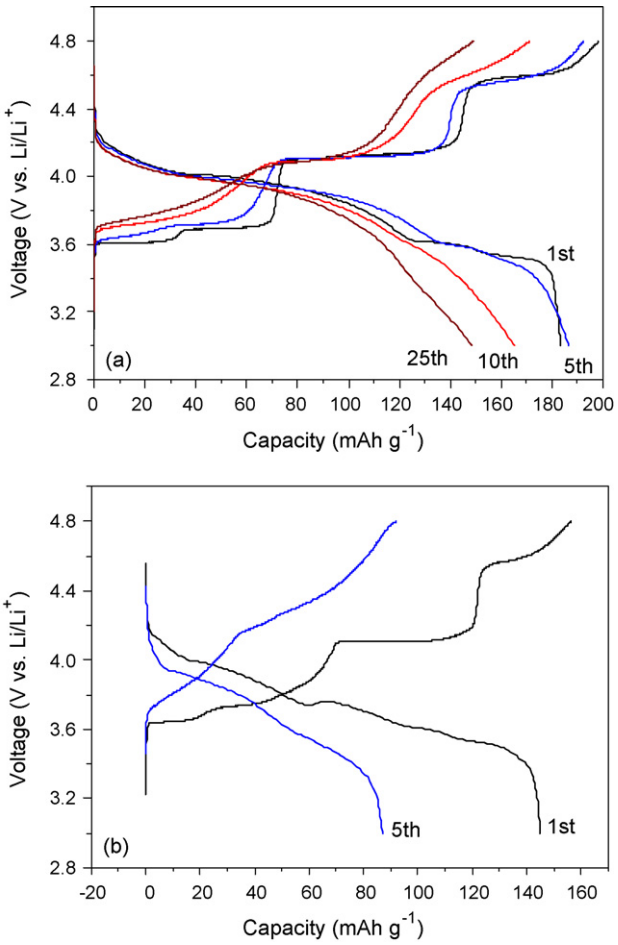

Fig. 8. Charge/discharge profiles of $Li_3V_2(PO_4)_3$ samples (a) MW5m and (b) CP10h with various cycles in the voltage range of 3.0–4.8 V.

in this large electrochemical window (3.0–4.8 V) [6]. Second, the as-synthesized samples $Li_3V_2(PO_4)_3$ without carbon coating might be a little dissolved under relative higher voltage, because a better carbon coating can keep off the contact of $Li_3V_2(PO_4)_3$ with electrolyte. Third, the crystal structure of $V_2(PO_4)_3$ and $LiV_2(PO_4)_3$ is distorted during the phase transition process at the high voltage (>4.6 V). Because of the electron/Li^+ location and transport within this lattice, the conductivity of $Li_3V_2(PO_4)_3$ sample without carbon coating might be increased during the extraction/reinsertion process which results in the poor cycleability presented.

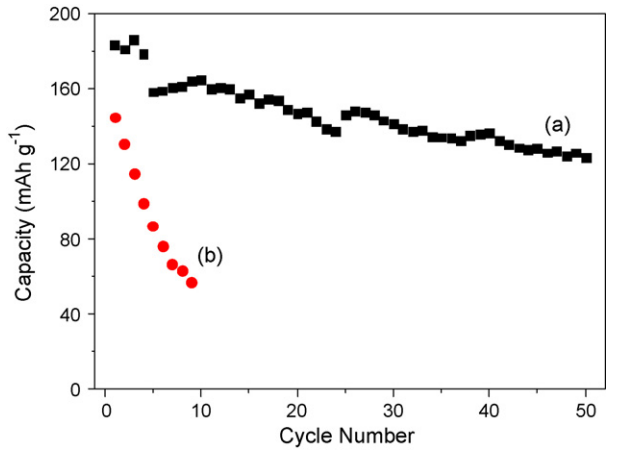

Fig. 9. Cyclic performance of the $Li_3V_2(PO_4)_3$ samples (a) MW5m and (b) CP10h in the voltage range of 3.0–4.8 V.

4. Conclusions

Monoclinic $Li_3V_2(PO_4)_3$ is rapidly synthesized at 750 °C for 5 min by using microwave solid-state synthesis method. The crystal growth of $Li_3V_2(PO_4)_3$ is dramatically accelerated in microwave irradiation field. The refined cell parameters and atomic coordinate of $Li_3V_2(PO_4)_3$ rapidly synthesized in microwave irradiation field show some deviations by comparison with those of $Li_3V_2(PO_4)_3$ synthesized in conventional solid-state synthesis method, especially the coordinates of Li atoms. It might be attributed to the strain in the particles and the dismatching coefficient diffusion of lithium ions with the formation of rigid framework by VO_6 and PO_4 polyhedra in microwave irradiation field, because of the too fast crystal growth process.

The carbon-free sample MW5m presents very well electrochemical properties. At the cut-off voltage of 3.0–4.3 V, MW5m presents a specific charge/discharge capacity of 132 and 126 mAh g^{-1}, respectively. There is a different plateau capacity of the $Li_3V_2(PO_4)_3$ samples synthesized upon conventional solid-state synthesis and microwave irradiation solid-state synthesis methods, respectively. One key control factor of specific capacity fade would be dependent on the phase transition process from $LiV_2(PO_4)_3$ to $LiV_2(PO_4)_3$ during the charge/discharge process of $Li_3V_2(PO_4)_3$ in the voltage range of 3.0–4.3 V. In the cut-off voltage of 3.0–4.8 V, the rapidly synthesized sample MW5m presents an initial specific charge and discharge capacity of 197 and 183.4 mAh g^{-1}.

However, compared with the good cycleability presented in the cut-off voltage of 3.0–4.3 V, the sample $Li_3V_2(PO_4)_3$without carbon coating presents a significant capacity loss in the cut-off voltage of 3.0–4.8 V. The capacity fade of $Li_3V_2(PO_4)_3$ is dependent on the cut-off voltage and the preparation method, more capacity lost at relatively higher charge/discharge voltage. It might be due to the fact that the carbon-free $Li_3V_2(PO_4)_3$ has a little dissolved under relative higher voltage, and the crystal structure of $V_2(PO_4)_3$ and $LiV_2(PO_4)_3$ is distorted during the phase transition process at the high voltage. The detailed crystal growth mechanism of $Li_3V_2(PO_4)_3$ and the relative electrochemical properties of $Li_3V_2(PO_4)_3$ synthesized under different microwave irradiation conditions would be discussed in the following paper.

Acknowledgments

The authors gratefully acknowledge the financial supports of Natural Science Foundation of Jiangsu Province of China (Grant No. BK2006537), Natural Science Foundation of Jiangsu Educational Department of China (Grant No. 06KJA43014), and Natural Science Foundation of China (Grant No. 10874021).

References

[1] C. Delmas, M. Maccario, L. Croguennec, F. Le-Cras, F. Weill, Nat. Mater. 7 (2008) 665.
[2] B. Ellis, W.H. Kan, W.R.M. Makahnouk, L.F. Nazar, J. Mater. Chem. 17 (2007) 3248.
[3] A.K. Padhi, K.S. Nanjundaswamy, J.B. Goodenough, J. Electrochem. Soc. 144 (1997) 1188.
[4] B. Kang, G. Ceder, Nature 458 (2009) 190.
[5] M.Y. Saidi, J. Barker, H. Huang, J.L. Sowyer, G. Adamson, J. Power Sources 119 (2003) 266.
[6] H. Hung, S.C. Yin, T. Kerr, N. Taylor, L.F. Nazar, Adv. Mater. 14 (2002) 1525.
[7] M.M. Ren, Z. Zhou, Y.Z. Li, X.P. Gao, J. Yan, J. Power Sources 162 (2006) 1357.
[8] Y.Z. Li, Z. Zhou, X.P. Gao, J. Yan, Electrochim. Acta 52 (2007) 4922.
[9] S.C. Yin, H. Grondey, P. Strobel, M. Anne, L.F. Nazar, J. Am. Chem. Soc. 125 (2003) 10402.
[10] P. Fu, Y.M. Zhao, Y.Z. Dong, X.N. An, G.P. Shen, J. Power Sources 162 (2006) 651.

[11] Q.Q. Chen, J.M. Wang, Z. Tang, W.C. He, H.B. Shao, J.Q. Zhang, Electrochim. Acta 52 (2007) 5251.
[12] M.M. Ren, Z. Zhou, X.P. Gao, W.X. Peng, J.P. Wei, J. Phys. Chem. C 112 (2008) 5689.
[13] S. Patoux, C. Wurm, M. Morcrette, G. Rousse, C. Masquelier, J. Power Sources 119 (2003) 278.
[14] J. Barker, P.K.B. Gover, P. Burns, A. Bryan, Electrochem. Solid-State Lett. 8 (2005) A285.
[15] H. Huang, T. Faulkner, J. Barker, M.Y. Saidi, J. Power Sources 189 (2009) 748.
[16] M.Y. Saidi, J. Barker, H. Huang, G. Adamson, Electrochem. Solid-State Lett. 5 (2002) A149.
[17] H. Ohkawa, K. Yoshida, M. Saito, K. Uematsu, K. Toda, M. Sato, Chem. Lett. (1999) 1017.
[18] J. Yang, J.J. Xu, J. Electrochem. Soc. 153 (2006) A716.
[19] M.R. Yang, W. Ke, S.H. Wu, J. Power Sources 165 (2007) 646.
[20] Y. Chen, Y.M. Zhao, X. An, J. Liu, Y. Dong, L. Chen, Electrochim. Acta 54 (2009) 5844.
[21] X.H. Rui, C. Li, C.H. Chen, Electrochim. Acta 54 (2009) 3374.
[22] J. Barker, M.Y. Saidi, J.L. Swoyer, et al., J. Electrochem. Soc. 150 (2003) A684.
[23] T. Jiang, C.Z. Wang, G. Chen, H. Chen, Y.J. Wei, X. Li, Solid State Ionics 180 (2009) 708.
[24] J.C. Zheng, X.H. Li, Z.X. Wang, H.J. Guo, Q.Y. Hu, W.J. Peng, J. Power Sources 189 (2009) 476.
[25] X.C. Zhou, Y.M. Liu, Y.L. Guo, Electrochim. Acta 54 (2009) 2253.
[26] M. Panneerselvam, K.J. Rao, Chem. Mater. 15 (2003) 2247.
[27] G. Yang, G. Wang, W.H. Hou, J. Phys. Chem. B 109 (2005) 11186.
[28] M. Higuchi, K. Katayama, Y. Azuma, M. Yukawa, M. Suhara, J. Power Sources 119 (2003) 258.
[29] K.S. Park, J.T. Sona, H.T. Chung, S.J. Kim, C.H. Lee, H.G. Kim, Electrochem. Commun. 5 (2003) 839.
[30] G.T. Zhou, O. Palchik, V.G. Pol, E. Sominski, Y. Koltypin, A. Gedanken, J. Mater. Chem. 13 (2003) 2607.
[31] G. Yang, Y. Kong, W.H. Hou, Q.J. Yan, J. Phys. Chem. B 109 (2005) 1371.
[32] T.A. Nissinen, Y. Kiros, M. Gasik, M. Leskela, Chem. Mater. 15 (2003) 4974.
[33] M. Nakayama, K. Watanabe, H. Ikuta, Y. Uchimoto, M. Wakihara, Solid State Ionics 164 (2003) 35.
[34] A.C. Larson, R.B. Von Dreele, General Structure Analysis System (GSAS), Los Alamos National Laboratory Report LAUR 2000, 86-748.
[35] I. Lopes, N.E. Hassan, H. Guerba, G. Wallez, A. Davidson, Chem. Mater. 18 (2006) 5826.
[36] D. Morgan, A. Van der Ven, G. Ceder, Electrochem. Solid-State Lett. 7 (2004) A30.
[37] M.S. Islam, D.J. Driscoll, C.A.J. Fisher, P.R. Slater, Chem. Mater. 17 (2005) 5085.